

## Research Article

# Radiolytic Synthesis of Pt-Ru Catalysts Based on Functional Polymer- Grafted MWNT and Their Catalytic Efficiency for CO and MeOH

Dae-Soo Yang, Kwang-Sik Sim, Hai-Doo Kwen, and Seong-Ho Choi

Department of Chemistry, Hannam University, Daejeon 305-811, Republic of Korea

Correspondence should be addressed to Seong-Ho Choi, shchoi@hnu.kr

Received 12 April 2010; Revised 4 June 2010; Accepted 23 June 2010

Academic Editor: William W. Yu

Copyright © 2011 Dae-Soo Yang et al. This is an open access article distributed under the Creative Commons Attribution License, which permits unrestricted use, distribution, and reproduction in any medium, provided the original work is properly cited.

Pt-Ru catalysts based on functional polymer-grafted MWNT (Pt-Ru@FP-MWNT) were prepared by radiolytic deposition of Pt-Ru nanoparticles on functional polymer-grafted multiwalled carbon nanotube (FP-MWNT). Three different types of functional polymers, poly(acrylic acid) (PAAc), poly(methacrylic acid) (PMAc), and poly(vinylphenyl boronic acid) (PVPBac), were grafted on the MWNT surface by radiation-induced graft polymerization (RIGP). Then, Pt-Ru nanoparticles were deposited onto the FP-MWNT supports by the reduction of metal ions using  $\gamma$ -irradiation to obtain Pt-Ru@FP-MWNT catalysts. The Pt-Ru@FP-MWNT catalysts were then characterized by XRD, XPS, TEM, and elemental analysis. The catalytic efficiency of Pt-Ru@FP-MWNT catalyst was examined for CO stripping and MeOH oxidation for use in a direct methanol fuel cell (DMFC). The Pt-Ru@PVPBac-MWNT catalyst shows enhanced activity for electro-oxidation of CO and MeOH oxidation over that of the commercial E-TEK catalyst.

## 1. Introduction

Although carbon-supported Pt-Ru nanoparticles (Pt-Ru/C) are known to be the best anode catalysts for direct methanol fuel cell (DMFC), they are still insufficient for the commercial application. Many researcher efforts have been devoted to improving the catalytic performance of Pt-Ru/C by catalyst dispersion [1–3]. In previous paper, we deposited Pt-Ru nanoparticles on the surface of the various carbon supports, including Vulcan XC-71, Ketjen-300, Ketjen-600, SWNTs, and MWNTs for use as fuel cell catalysts [4]. However, the metallic alloy nanoparticles were aggregated on the surface of the carbon supports due to their hydrophobic nature. The metal (Ag or Pd) and alloy (Pt-Ru) nanoparticles were also deposited on the surface of single-walled carbon nanotubes (SWNTs) [5], and porous carbon supports using  $\gamma$ -irradiation without protecting agents [6]. Silva et al. [7] reported the preparation of Pt-Ru/C electrocatalysts using  $\gamma$ -irradiation in water/ethylene glycol. This paper showed the patterns of Pt-Ru nanoparticles on carbon supports; however, it did not indicate the catalytic efficiency of MeOH oxidation based on the aggregation degree. It is proposed that

the catalytic efficiency is affected by the metallic nanoparticle aggregation degree on carbon supports.

To overcome the aggregation of the metallic nanoparticles, the carbon support surface was modified with hydrophobic properties to obtain hydrophilic properties by *in-situ* polymerization of  $\beta$ -caprolactone, methacrylate, and pyrrole using oxidizing agents as the initiator [8]. Pt-Ru nanoparticles were then deposited on the polymer-wrapped MWNT supports to produce a direct methanol fuel cell (DMFC) catalyst. Pt-Ru at poly(pyrrole)-MWNT catalysts obtained high catalytic efficiency for CO stripping and methanol oxidation. The surface of MWNTs was then coated using conductive polymers such as aniline, pyrrole, and thiophene to go from hydrophobic properties to hydrophilic properties [9]. Finally, the metallic nanoparticles were deposited on conducting polymer-wrapped MWNTs. However, the prepared Pt-Ru catalysts provided lower catalytic efficiency compared to that of commercial E-TEK catalyst.

Radiation-induced graft polymerization (RIGP) is a useful method for the introduction of functional groups onto different polymer materials using specially selected monomers. There have been several reports about RIGP

of polar monomers onto polymer substrates to obtain hydrophilic properties for versatile applications [10–14]. The RIGP method can easily functionalize the surface of MWNTs to the desired properties. In a previous paper, we described the functionalization of MWNTs by RIGP of derivatives vinyl monomers and their application in enzyme-free biosensors [15]. However, little has been reported about the deposition of Pt-Ru nanoparticles on the functionalized MWNT supports by  $\gamma$ -irradiation for DMFC catalysts.

In this study, Pt-Ru nanoparticles were deposited on the functional polymer (FP)-grafted MWNT obtained from RIGP using  $\gamma$ -irradiation to produce an anode catalyst for DMFCs. The obtained Pt-RuatFP-MWNT catalysts were characterized by XRD, XPS, TEM, and elemental analysis. Furthermore, the catalytic efficiency of the Pt-RuatFP-MWNT catalyst was evaluated for CO stripping and MeOH oxidation for use in a DMFC and compared to the catalytic efficiency of the commercial E-TEK catalyst.

## 2. Experimental

**2.1. Chemicals.**  $\text{H}_2\text{PtCl}_6 \times \text{H}_2\text{O}$  (37.5% Pt),  $\text{RuCl}_3 \times \text{H}_2\text{O}$  (41.0% Ru), acrylic acid (AAc), methacrylic acid (MAc), and 4-vinylphenylboronic acid (VPBAc) were of analytical reagent grade (Sigma-Aldrich, USA) and used without further purification. MWNTs (CM-95) were supplied by Hanwha Nanotech Co., Ltd (Korea). The commercial E-TEK catalyst (metallic content, 30 wt-%) was purchased from E-TEK (BASF Fuel Cell Inc., NJ, USA). Nafion (perfluorinated ion-exchange resin, 5% (w/v) solution in a solution of 90% aliphatic alcohol/10% water mixture) was also purchased from Sigma-Aldrich (USA). Solutions for the experiments were prepared with water purified in a Milli-Q puls water purification system (Millipore Co. Ltd. USA), the final resistance of water was  $18.2 \text{ M}\Omega\text{cm}^{-1}$  and degassed prior to each measurement. Other chemicals were of reagent grade.

**2.2. RIGP of Functional Monomers on the Surface of MWNTs.** MWNTs were purified to remove the catalyst and noncrystallized carbon impurities with phosphoric acid solution. The purified MWNTs were used as the supporting materials for grafting of various vinyl monomers. The MWNTs (2.0 g) and AAc (2.0 g) were then mixed in aqueous solution (20 mL). Nitrogen gas was bubbled through the solution for 30 minutes to remove oxygen gas, and the solution was irradiated from a Co-60 source under atmospheric pressure and ambient temperature. A total irradiation dose of 30 kGy (dose rate =  $6.48 \times 10^5/\text{h}$ ) was used. The other functional polymer-grafted MWNTs were prepared using a similar procedure.

**2.3. Preparation of Pt-RuatFP-MWNT Catalysts by  $\gamma$ -Irradiation.** The Pt-RuatPVPBAc-MWNT catalysts were prepared as follows:  $\text{H}_2\text{PtCl}_6 \times \text{H}_2\text{O}$  (0.43 g) and  $\text{RuCl}_3 \times \text{H}_2\text{O}$  (0.41 g) were dissolved in deionized water (188 mL) in 2-propanol (12.0 mL) as the radical scavenger. 1.00 g of PVPBAc-MWNT support was added to the above solution. Nitrogen was bubbled for 30 min through the solution to remove oxygen and then irradiated under atmospheric

pressure and ambient temperature. A total irradiation dose of 30 kGy (a dose rate =  $6.48 \times 10^5/\text{h}$ ) was applied. Pt-Ru nanoparticle-deposited PVPBAc-MWNT catalysts were precipitated after  $\gamma$ -irradiation. The Pt-RuatPAAc-MWNT and Pt-RuatPMAc-MWNT catalysts were prepared as described above.

**2.4. Characteristics of Pt-RuatFP-MWNT Catalysts.** Particle size and morphology of the Pt-RuatFP-MWNT catalysts were analyzed by HR-TEM (JEOL, JEM-2010, USA). The content of Pt and Ru in samples was analyzed by inductively coupled plasma-atomic emission spectrometer (ICP-AES) (Jobin-Yvon, Ultima-C, USA). X-ray diffraction (XRD) patterns for samples were obtained using a Japanese Rigaku D/max  $\gamma\text{A}$  X-ray diffractometer equipped with graphite monochromatized Cu K $\alpha$  radiation ( $\lambda = 0.15414 \text{ nm}$ ). The scanning range was  $5\text{--}80^\circ$  with a scanning rate of  $5^\circ/\text{min}$ .

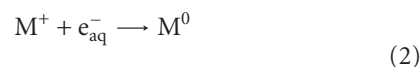
To evaluate the catalytic efficiency of Pt-RuatFP-MWNT catalysts for the electro-oxidation of CO and MeOH, the Pt-RuatFP-MWNT-coated electrode was prepared as follows. Firstly, the catalytic inks were prepared by mixing of Pt-RuatFP-MWNT catalysts (5.0 mg) and 5% Nafion solution (0.05 mL) and stirred for 24 hrs. Secondly, the catalytic inks were applied on a glass carbon ( $0.02 \text{ cm}^2$ ) by wet coating and dried in a vacuum oven at  $50^\circ\text{C}$  under nitrogen gas. The electro-oxidation of CO and MeOH (1.0 M) was examined using the Pt-RuatFP-MWNT catalyst electrode, submerged in 0.5 M  $\text{H}_2\text{SO}_4$  electrolyte by cyclic voltammetry (EG&G Instruments, Potentiostat/Galvanostat model 283, USA) at scan rate of 100 mV/s. All the measurements were carried out at room temperature.

## 3. Results and Discussion

**3.1. Radiolytic Preparation of Pt-RuatFP-MWNT Catalysts and Its Characterization.** Pt-RuatFP-MWNT catalysts were prepared by radiolytic reduction of metallic ions in water/2-propanol solution in the presence of FP-MWNT supports at room temperature. When  $\gamma$ -ray irradiated in aqueous solutions, various species were generated, as shown in the following equation [16]:



Among them, the solvated electrons,  $e_{\text{aq}}^-$  and  $\text{H}^\cdot$  radicals can be used as strong reducing agents. The metal ions were reduced to the zero-valent state as shown in the following:



Similarly, multivalent ions, such as  $\text{Pt}^{4+}$  and  $\text{Ru}^{3+}$ , are reduced by a multistep reaction. On the other hand, the hydroxyl radical ( $\text{OH}^\cdot$ ) can be oxidized for the ions or zero-valence metal atom. In order to protect the oxidizing agent ( $\text{OH}^\cdot$ ), 2-propanol was added to the reaction solution. The  $\text{OH}^\cdot$  radical was reacted with 2-propanol as shown in (3). As

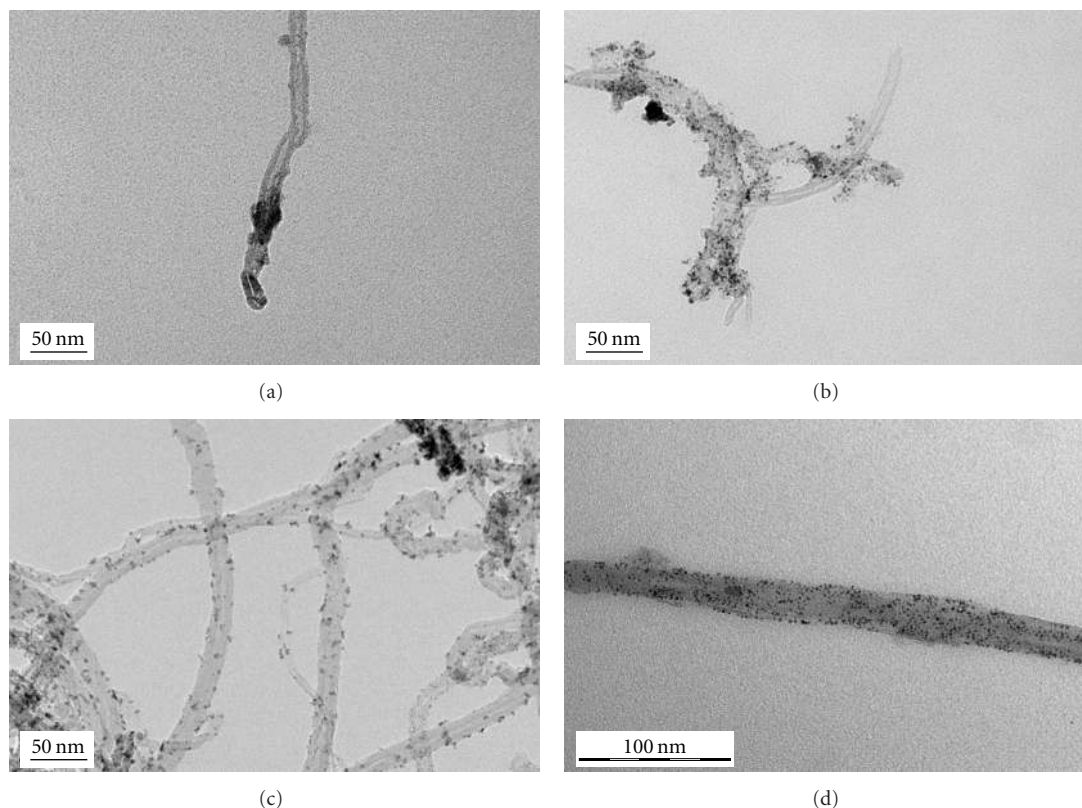


FIGURE 1: TEM images of the Pt-Ru/MWNT (a), Pt-Ru/PAAc-MWNT (b), Pt-Ru/PMAC-MWNT (c) and Pt-Ru/PVPBAC-MWNT (d) catalyst prepared by  $\gamma$ -irradiation.

results, the metal ion was then reduced to zero-valence metal atom by 2-propanol radical as shown in the following.

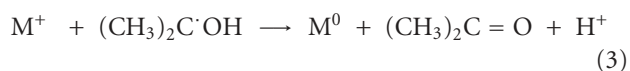


Figure 1 shows the TEM images of the Pt-Ru/MWNT (a), Pt-Ru/PAAc-MWNT (b), Pt-Ru/PMAC-MWNT (c), and Pt-Ru/PVPBAC-MWNT (d) catalysts prepared by  $\gamma$ -irradiation. As shown in Figure 1(a), there are no Pt-Ru nanoparticles on the surface of MWNT, whereas large amounts of Pt-Ru nanoparticles are shown on the surface of FP-MWNT supports, Figures 1(b), 1(c), and 1(d). Large amounts of Pt-Ru nanoparticles were successfully loaded on the surface of FP-MWNT. The mean particle sizes of the Pt-Ru nanoparticle on the surface of PAAc-MWNT, PMAC-MWNT, and PVPBAC-MWNT supports were in the range of 2.5–4.0 nm, 5.0–7.5 nm, and 2.0–2.5 nm, respectively. On the other hand, the commercial E-TEK catalyst showed a mean particle size of  $2.5 \pm 0.7$  nm [17]. As shown in the TEM image, the Pt-Ru nanoparticles were well dispersed on the surface of FP-MWNT supports because the surface of carbon is changed from hydrophobic property to hydrophilic property. The property of metallic nanoparticles was also possessed as hydrophilic property. Thus, these catalysts are expected to have good efficiency for methanol oxidation.

To clarify the chemical state of Pt-Ru nanoparticles deposited on FP-MWNTs, X-Ray photoelectron spectroscopy (XPS) measurements were taken. Figure 2 shows the regional  $\text{Pt}_{4f}$  and  $\text{Ru}_{3p}$  XPS spectra of Pt-Ru/PAAc-MWNT (a), Pt-Ru/PMAC-MWNT (b), and Pt-Ru/PVPBAC-MWNT catalyst (c) prepared by  $\gamma$ -irradiation. The  $\text{Pt}_{4f}$  peaks of the catalysts appeared about 72 eV and 75 eV due to metallic Pt and  $\text{Pt(IV)O}_2$ , respectively. Li and Hsing [18] reported that the  $\text{Pt}_{4f}$  XPS signal was appeared into three components with respective binding energies of 71.8, 72.9, and 74.6 eV. It was concluded that these signals were attributed to the metallic Pt,  $\text{Pt(II)O}$ , and  $\text{Pt(IV)O}_2$  species. On the other hand, the  $\text{Ru}_{3p_{1/2}}$  and  $\text{Ru}_{3p_{3/2}}$  peaks for the Pt-Ru/PAAc-MWNT and Pt-Ru/PMAC-MWNT were shown at 486 eV and 463 eV, respectively. The 463 eV signals are due to metallic Ru(0). Li and Hsing [18] interpreted 463 eV signal due to Ru(0) and  $\text{RuO}_2$ . In Figure 2(c), the  $\text{Ru}_{3p}$  signals of Pt-Ru/PVPBAC-MWNT catalysts were shifted onto the large binding energy compared to that of Pt-Ru/PAAc-MWNT and Pt-Ru/PMAC-MWNT. It may be considered that the hydrous ruthenium oxide,  $\text{RuO}_x\text{Hy}$ , was produced from the reaction of boronic acid group of the grafted PVPBAC onto MWNT during  $\gamma$ -irradiation. However, a further investigation is needed to clarify these signals.

Figure 3 shows the X-ray diffraction patterns of the Pt-Ru/FP-MWNT catalysts prepared by  $\gamma$ -irradiation. All samples showed the peak at about  $20^\circ$ , which was associated

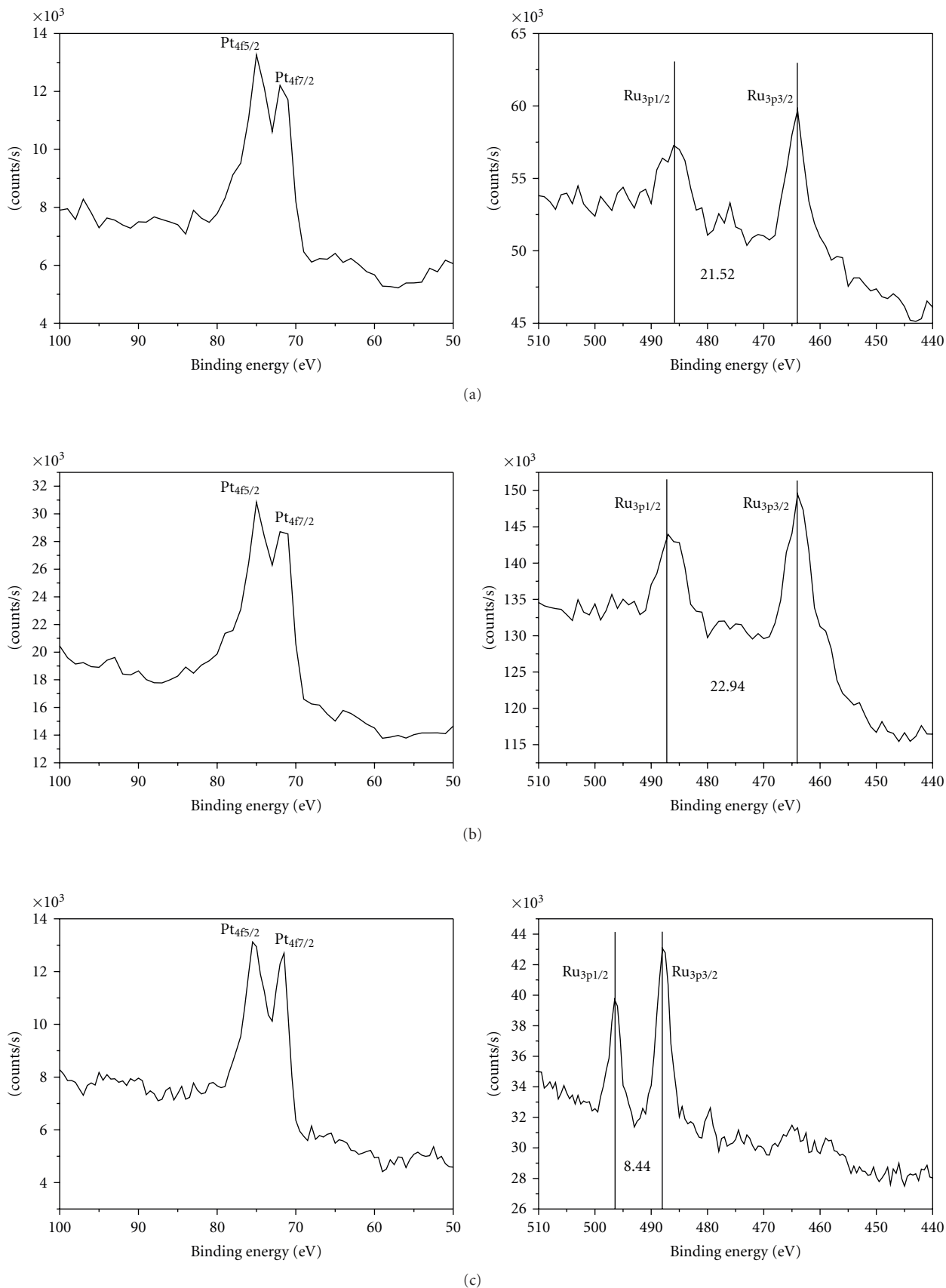


FIGURE 2: X-ray photoelectron spectroscopy (XPS) spectra of Pt and Ru on Pt-RuatPAAc-MWNT (a), Pt-RuatPMAc-MWNT (b) and Pt-RuatPVBAc-MWNT catalyst (c) prepared by  $\gamma$ -irradiation.

TABLE 1: Contents of Pt-Ru on the prepared catalyst<sup>(a)</sup>.

Catalysts	Pt content(wt-%)	Ru content (wt-%)
Pt-Ru at MWNT	ND	ND
Pt-Ru at PAAc-MWNT	8.77	10.8
Pt-Ru at PMAc-MWNT	8.20	9.98
Pt-Ru at PVPBac-MWNT	<b>11.2</b>	<b>6.01</b>
E.TEK catalyst(30 wt-%)	21.6	10.5

<sup>(a)</sup> Metal content (wt-%) was determined by ICP-AES.

to the MWNT supporting material. The crystallinity of Pt-Ru catalysts was confirmed by the presence of peaks around  $39.9^\circ$ ,  $46.2^\circ$ , and  $67.4^\circ$ . These peaks are assigned as Pt(111), (200) planes, and (220), respectively, of the face-centered cubic (fcc) structure of platinum and platinum alloy particles [19]. The XRD peaks corresponding to metallic ruthenium with hexagonal structure were not detected for these samples. The average particle size of the Pt-Ru catalysts can be calculated via XRD patterns according to Scherrer's formula [20, 21].

$$d_{\text{XRD}} = \frac{0.9\lambda}{\beta_{1/2} \cos \theta}, \quad (4)$$

where  $d_{\text{XRD}}$  is the average particle size (nm)  $\lambda$  is the wavelength of the  $x$ -ray (0.15406 nm)  $\theta$  is the angle at the peak maximum  $\beta_{1/2}$  is the width (radians) of the peak at half height. The calculated mean sizes from the diffraction peak of Pt(111) are as follows: 3.2 nm in Figure 3(a), 3.1 nm in Figure 3(b), and 2.9 nm in Figure 3(c). There are no size changes of Pt-Ru catalyst on various functionalized polymer-grafted MWNT. This behavior may show that the growth of nanoparticles is prevented via dimethylketone during  $\gamma$ -irradiation, as shown in (5).

Table 1 shows the content (wt-%) of Pt and Ru elements in the Pt-Ru at FP-MWNT catalysts. In ICP-AES results of the Pt-Ru at FP-MWNT catalyst, the Pt element content (wt-%) in the Pt-Ru at PAAc-MWNT, Pt-Ru at PMAc-MWNT, and Pt-Ru at PVPBac-MWNT catalysts was determined as 8.77%, 8.20%, and 11.20% for all that addition of 16.125% in reaction mixture, respectively. While Ru element content in the Pt-Ru at PAAc-MWNT, Pt-Ru at PMAc-MWNT, and Pt-Ru at PVPBac-MWNT catalysts was obtained as 10.8%, 9.98%, and 6.01%, for all that addition of 16.81% in reaction mixture, respectively. In the case of Pt-Ru at PVPBac-MWNT catalyst, the Pt content is higher than that of the other catalysts. In commercial E-TEK catalyst, the Pt content is higher than Ru content, as shown in Table 1.

**3.2. Catalytic Efficiency of Pt-Ru at FP-MWNT Catalyst for CO and MeOH.** To find the catalytic efficiency of Pt-Ru at FP-MWNT catalysts, they were tested for the electrochemical oxidation of carbon monoxide (CO). Figure 4 shows the cyclic voltammograms (CVs) of electro-oxidation of CO for Pt-Ru at FP-MWNT catalyst prepared by  $\gamma$ -irradiation

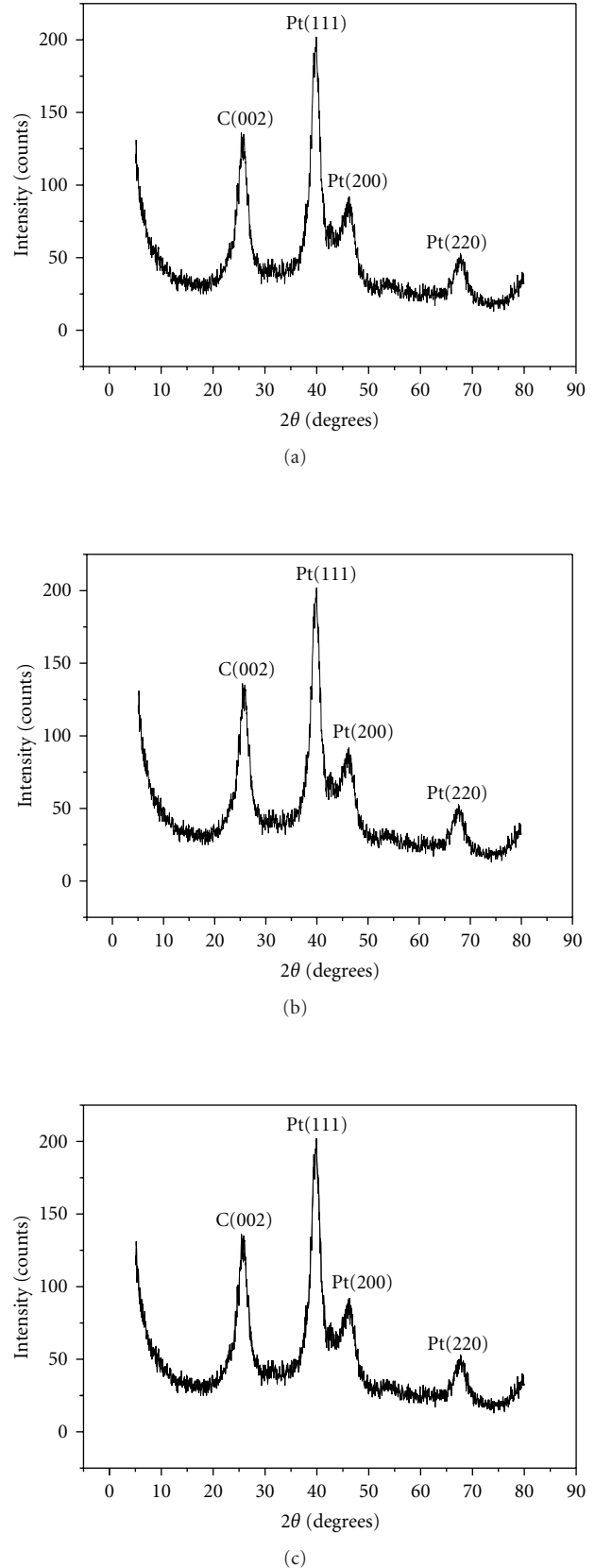


FIGURE 3: XRD spectra of Pt-Ru at PAAc-MWNT (a), Pt-Ru at PMAc-MWNT (b), and Pt-Ru at PVPBac-MWNT (c) catalyst for DMFC.

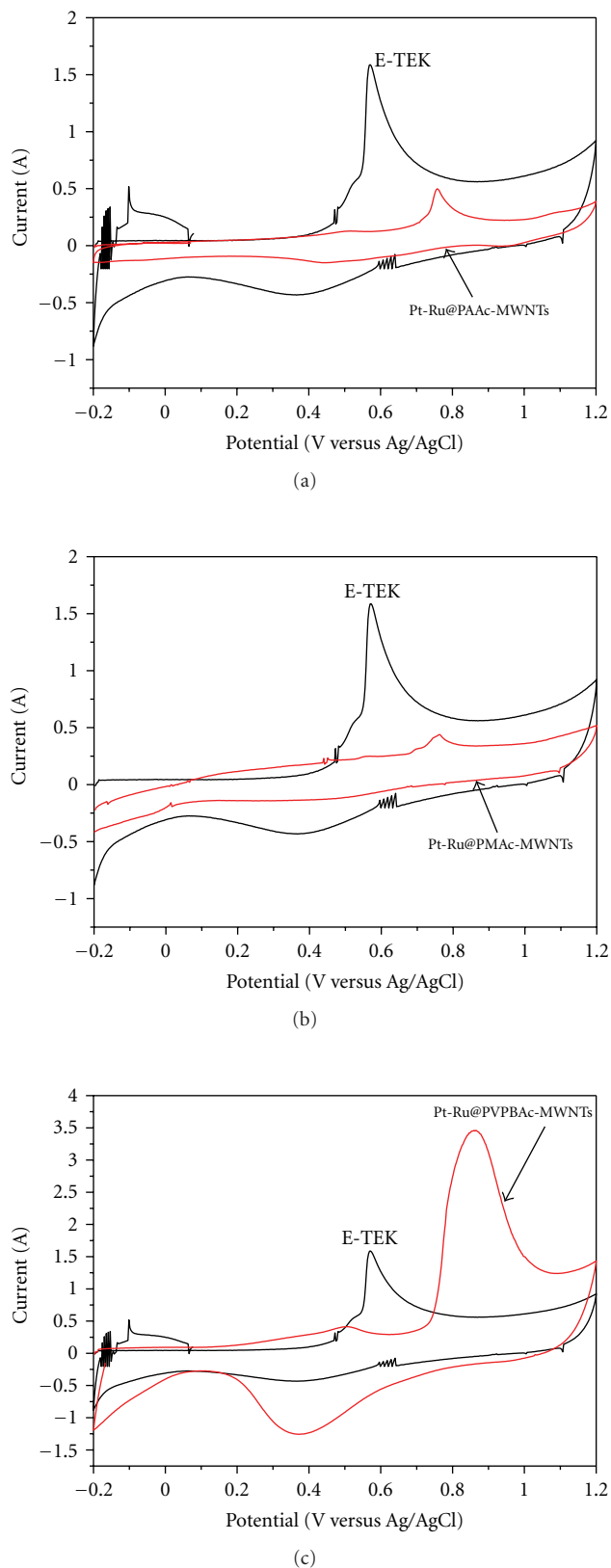


FIGURE 4: Comparison of CO adsorption efficiency in 0.5 M  $\text{H}_2\text{SO}_4$  between E-TEK the catalyst and the prepared catalyst. (a) E-TEK catalyst versus Pt-RuatPAAc-MWNT catalyst, (b) E-TEK catalyst versus Pt-RuatPMAc-MWNT, (c) E-TEK versus Pt-RuatPVPBac-MWNT.

in 0.5 M  $\text{H}_2\text{SO}_4$ : (a) RuatPAAc-MWNT, (b) Pt-RuatPMAc-MWNT, and (c) Pt-RuatPVPBac-MWNT catalyst. To compare CO adsorption efficiency, it was measured and compared to the commercial E-TEK catalyst containing 30 wt% Pt on carbon. The higher CO stripping peak at the commercial E-TEK catalyst electrode is more apparent than that of the Pt-RuatPAAc-MWNT and Pt-RuatPMAc-MWNT catalyst electrodes, as shown in Figures 4(a) and 4(b). However, the measured CO stripping peak at Pt-RuatPVPBac-MWNT catalyst electrode is significantly higher than that of the commercial E-TEK electrode in spite of the metal catalyst in high amount as shown in Figure 4(c). A significant current density is noticed at the Pt-RuatPVPBac-MWNT catalyst electrodes for the CO oxidation starting from 0.72 V. The electrochemically active specific area (SEAS) of the catalysts was calculated using the charges deduced from the CV of CO adsorption and desorption electro-oxidation process and using (5) [22].

$$\text{SEAS} = \frac{Q_{\text{CO}}}{G} \times 420, \quad (5)$$

where  $Q_{\text{CO}}$  is the charge for CO desorption electro-oxidation in microcoulomb ( $\mu\text{C}$ );  $G$  represents the summation of Pt + Ru metals loading ( $\mu\text{g}$ ) in the electrode, and 420 is the charge required to oxidize a monolayer of CO on the catalysts in  $\mu\text{C cm}^{-2}$ . The electrochemical SEASs are  $60 \text{ m}^2 \text{ g}^{-1}$  for the commercial E-TEK catalysts. In the case of the prepared catalysts, the electrochemical SEASs are 34, 30, and  $126 \text{ m}^2 \text{ g}^{-1}$  for the Pt-RuatPAAc-MWNT, Pt-RuatPMAc-MWNT, and Pt-RuatPVPBac-MWNT catalysts, respectively. The SEAS of Pt-RuatPVPBac-MWNT catalysts prepared by  $\gamma$ -irradiation are higher than that of commercial E-TEK catalysts due to hydrous ruthenium oxide. It might be based on the promotion of CO oxidation on Pt atoms by the second metal (Ru) which provides OH-type species, the more oxidizable second metal, thus promotes catalytic activities.

Figure 5 shows the cyclic voltammograms of E-TEK catalyst and the prepared catalysts for 1.0 M MeOH oxidation in 0.5 M  $\text{H}_2\text{SO}_4$  at room temperature. The higher current peak at about 0.6 V versus Ag/AgCl electrode appeared due to methanol oxidation on the commercial E-TEK catalyst, as shown in Figures 5(a), 5(b), and 5(c). However, the methanol oxidation peak for Pt-RuatPAAc-MWNT catalyst and Pt-RuatPMAc-MWNT catalyst were lower than that of the E-TEK catalyst, as shown in Figures 5(a) and 5(b). In the case of Pt-RuatPVPBac-MWNT catalyst, the large catalytic efficiency at 0.8 V was observed. As a result, the prepared Pt-RuatPVPBac-MWNT catalyst can be used on a direct methanol fuel cell electrode.

#### 4. Conclusion

The functionalized MWNTs were prepared by radiation-induced graft polymerization of vinyl monomers with the desired functional group. Subsequently, Pt-Ru nanoparticles were deposited on the surface of the functionalized MWNT for using as a fuel cell-electrode catalyst. The efficiency

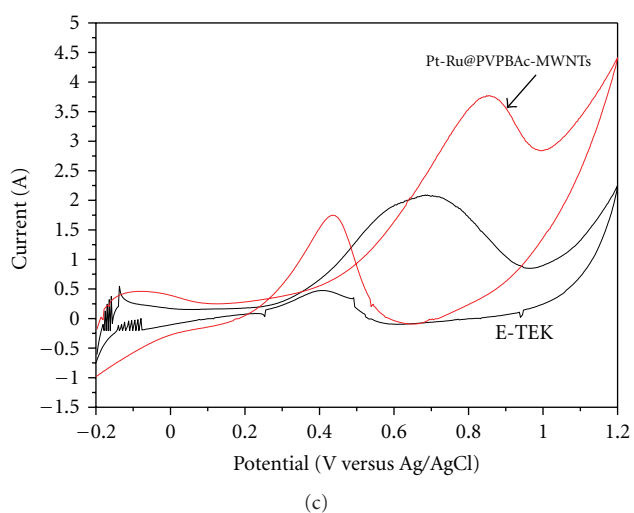
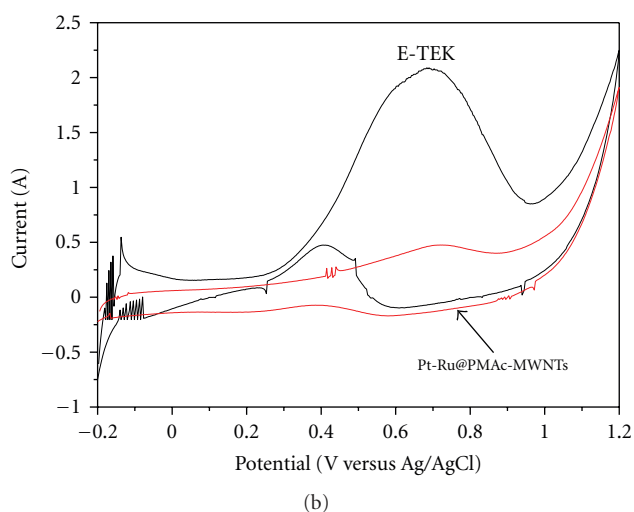
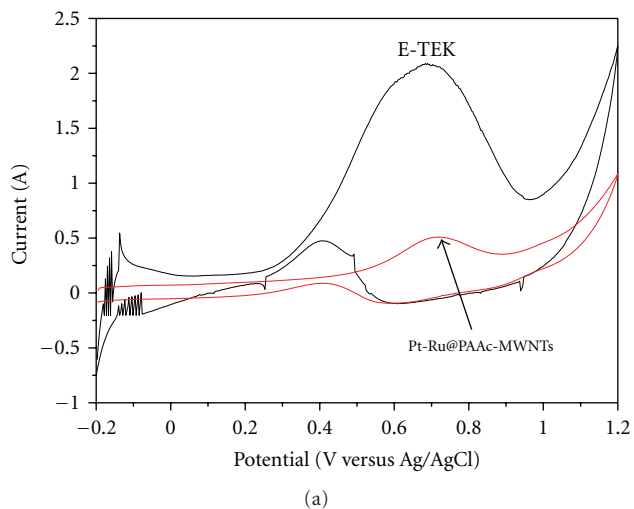


FIGURE 5: Comparison of catalytic efficiency among E-TEK catalyst and the prepared catalysts for MeOH oxidation in 0.5 M  $\text{H}_2\text{SO}_4$ . E-TEK catalyst versus Pt-Ru@PAAc-MWNT catalyst, (b) E-TEK catalyst versus Pt-Ru@PMAc-MWNT catalyst, and (c) E-TEK catalyst versus Pt-Ru@PVPBAC-MWNT.

of the prepared catalysts was investigated. The following conclusions are based on the results.

- (1) The catalytic efficiency of Pt-Ru@PVPBAC-MWNT catalyst for CO stripping was higher than that of the commercial E-TECK catalyst in spite of the low metallic content.
- (2) The stripping voltammograms for the adsorbed CO at Pt-Ru@PVPBAC-MWNT catalyst prepared by  $\gamma$ -irradiation reveal that the CO oxidation is energetically favorable at these electrodes.
- (3) The MeOH oxidation peak appeared at 0.8 V on Pt-Ru@PVPBAC-MWNT catalyst prepared by  $\gamma$ -irradiation which appears to be suitable for the electrode assembly in direct methanol fuel cells.

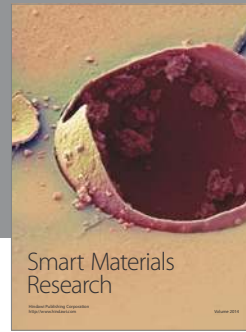
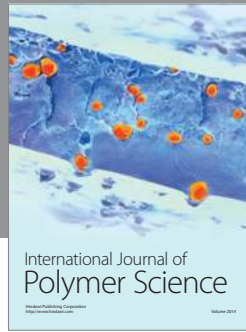
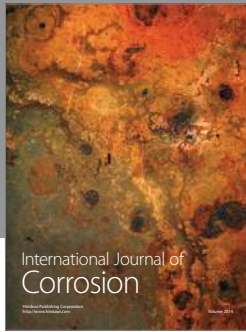
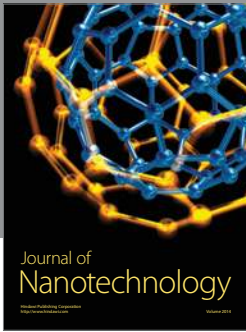
## Acknowledgments

This paper was supported by Nano R&D program and National Nuclear Technology program through the Korea Science and Engineering Foundation funded by the Ministry of Science & Technology. The authors particularly thank the Korea Basic Science Institute (KBSI) for FETEM measurements.

## References

- [1] B. Yang, Q. Lu, Y. Wang et al., "Simple and low-cost preparation method for highly dispersed PtRu/C catalysts," *Chemistry of Materials*, vol. 15, no. 18, pp. 3552–3557, 2003.
- [2] Z. Liu, X. Y. Ling, X. Su, and J. Y. Lee, "Carbon-supported Pt and PtRu nanoparticles as catalysts for a direct methanol fuel cell," *Journal of Physical Chemistry B*, vol. 108, no. 24, pp. 8234–8240, 2004.
- [3] G. Girishkumar, K. Vinodgopal, and P. V. Kamat, "Carbon nanostructures in portable fuel cells: single-walled carbon nanotube electrodes for methanol oxidation and oxygen reduction," *Journal of Physical Chemistry B*, vol. 108, no. 52, pp. 19960–19966, 2004.
- [4] S.-D. Oh, K. R. Yoon, S.-H. Choi et al., "Dispersion of Pt-Ru alloys onto various carbons using  $\gamma$ -irradiation," *Journal of Non-Crystalline Solids*, vol. 352, no. 4, pp. 355–360, 2006.
- [5] S.-D. Oh, B.-K. So, S.-H. Choi et al., "Dispersing of Ag, Pd, and Pt-Ru alloy nanoparticles on single-walled carbon nanotubes by  $\gamma$ -irradiation," *Materials Letters*, vol. 59, no. 10, pp. 1121–1124, 2005.
- [6] K.-D. Seo, S.-D. Oh, S.-H. Choi, S.-H. Kim, H. G. Park, and Y. P. Zhang, "Radiolytic loading of the Pt-Ru nanoparticles onto the porous carbons," *Colloids and Surfaces A*, vol. 313–314, pp. 393–397, 2008.
- [7] D. F. Silva, A. O. Neto, E. S. Pino, M. Linardi, and E. V. Spinacé, "PtRu/C electrocatalysts prepared using  $\gamma$ -irradiation," *Journal of Power Sources*, vol. 170, no. 2, pp. 303–307, 2007.
- [8] H.-B. Bae, J.-H. Ryu, B.-S. Byun, S.-H. Choi, S.-H. Kim, and C.-G. Hwang, "Radiolytic deposition of Pt-Ru catalysts on the conductive polymer coated MWNT and their catalytic efficiency for CO and MeOH," *Advanced Materials Research*, vol. 47–50, part 2, pp. 1478–1481, 2008.
- [9] H.-B. Bae, S.-H. Oh, J.-C. Woo, and S.-H. Choi, "Preparation of Pt-Ru@PPy-MWNT catalysts by  $\gamma$ -irradiation and chemical

- reduction and their adsorption capacity for CO," *Journal Nanoscience and Nanotechnology*, vol. 10, pp. 6901–6906, 2010.
- [10] S.-H. Choi, Y. C. Nho, and G.-T. Kim, "Adsorption of  $Pb^{2+}$  and  $Pd^{2+}$  on polyethylene membrane with amino group modified by radiation-induced graft copolymerization," *Journal of Applied Polymer Science*, vol. 71, no. 4, pp. 643–650, 1999.
- [11] S.-H. Choi and Y. C. Nho, "Adsorption of  $Co^{2+}$  by styrene-g-polyethylene membrane bearing sulfonic acid groups modified by radiation-induced graft copolymerization," *Journal of Applied Polymer Science*, vol. 71, no. 13, pp. 2227–2235, 1999.
- [12] S.-H. Choi and Y. C. Nho, "Adsorption of  $UO_2^{2+}$  by polyethylene adsorbents with amidoxime, carboxyl, and amidoxime/carboxyl group," *Radiation Physics and Chemistry*, vol. 57, no. 2, pp. 187–193, 2000.
- [13] S.-H. Choi and Y. C. Nho, "Radiation-induced graft copolymerization of binary monomer mixture containing acrylonitrile onto polyethylene films," *Radiation Physics and Chemistry*, vol. 58, no. 2, pp. 157–168, 2000.
- [14] S.-H. Choi, K.-P. Lee, and J.-G. Lee, "Adsorption behavior of urokinase by polypropylene film modified with amino acids as affinity groups," *Microchemical Journal*, vol. 68, no. 2-3, pp. 205–213, 2001.
- [15] D.-S. Yang, D.-J. Jung, and S.-H. Choi, "One-step functionalization of multi-walled carbon nanotubes by radiation-induced graft polymerization and their application as enzyme-free biosensors," *Radiation Physics and Chemistry*, vol. 79, no. 4, pp. 434–440, 2010.
- [16] J. Belloni, M. Mostafavi, H. Remita, J.-L. Marignier, and M.-O. Delcourt, "Radiation-induced synthesis of mono- and multi-metallic clusters and nanocolloids," *New Journal of Chemistry*, vol. 22, no. 11, pp. 1239–1255, 1998.
- [17] A. O. Neto, T. R. R. Vasconcelos, R. W. R. V. da Silva, M. Linardi, and E. V. Spinacé, "Electro-oxidation of ethylene glycol on PtRu/C and PtSn/C electrocatalysts prepared by alcohol-reduction process," *Journal of Applied Electrochemistry*, vol. 35, no. 2, pp. 193–198, 2005.
- [18] X. Li and I.-M. Hsing, "Surfactant-stabilized PtRu colloidal catalysts with good control of composition and size for methanol oxidation," *Electrochimica Acta*, vol. 52, no. 3, pp. 1358–1365, 2006.
- [19] M. Tsuji, M. Kubokawa, R. Yano et al., "Fast preparation of PtRu catalysts supported on carbon nanofibers by the microwave-polyol method and their application to fuel cells," *Langmuir*, vol. 23, no. 2, pp. 387–390, 2007.
- [20] Y. Shao, G. Yin, Y. Gao, and P. Shi, "Durability study of PtC and PtCNTs catalysts under simulated PEM fuel cell conditions," *Journal of the Electrochemical Society*, vol. 153, no. 6, pp. A1093–A1097, 2006.
- [21] S. Kim and S.-J. Park, "Effects of chemical treatment of carbon supports on electrochemical behaviors for platinum catalysts of fuel cells," *Journal of Power Sources*, vol. 159, no. 1, pp. 42–45, 2006.
- [22] A. Pozio, M. de Francesco, A. Cemmi, F. Cardellini, and L. Giorgi, "Comparison of high surface Pt/C catalysts by cyclic voltammetry," *Journal of Power Sources*, vol. 105, no. 1, pp. 13–19, 2002.



**Hindawi**

Submit your manuscripts at  
<http://www.hindawi.com>

